



HAL
open science

How disruption of endo-epicardial electrical connections enhances endo-epicardial conduction during atrial fibrillation

Ali Gharaviri, Sander Verheule, Jens Eckstein, Mark Potse, Pawel Kuklik,
Nico H.L. Kuijpers, Ulrich Schotten

► **To cite this version:**

Ali Gharaviri, Sander Verheule, Jens Eckstein, Mark Potse, Pawel Kuklik, et al.. How disruption of endo-epicardial electrical connections enhances endo-epicardial conduction during atrial fibrillation. 2016. hal-01386915

HAL Id: hal-01386915

<https://inria.hal.science/hal-01386915>

Preprint submitted on 5 Dec 2016

HAL is a multi-disciplinary open access archive for the deposit and dissemination of scientific research documents, whether they are published or not. The documents may come from teaching and research institutions in France or abroad, or from public or private research centers.

L'archive ouverte pluridisciplinaire **HAL**, est destinée au dépôt et à la diffusion de documents scientifiques de niveau recherche, publiés ou non, émanant des établissements d'enseignement et de recherche français ou étrangers, des laboratoires publics ou privés.



Distributed under a Creative Commons Attribution - NonCommercial - ShareAlike 4.0 International License

1 **How Disruption of Endo-epicardial Electrical Connections**
2 **Enhances Endo-epicardial Conduction during Atrial Fibrillation**

3 Ali Gharaviri Msc,¹ Sander Verheule PhD,¹ Jens Eckstein MD, PhD,^{1,4} Mark Potse PhD,^{2,3} Pawel
4 Kuklik,¹ Nico H.L. Kuijpers PhD,² Ulrich Schotten MD, PhD¹

5 1: Dept. of Physiology, Maastricht University, Maastricht, The Netherlands.

6 2: Dept. of Biomedical Engineering, Maastricht University, Maastricht, The Netherlands.

7 3: Institute of Computational Science, Faculty of Informatics, Università della Svizzera, italiana,
8 Lugano, Switzerland.

9 4: University Hospital Basel, Dept. of Internal Medicine, Basel, Switzerland.

10 Institution where work was done: Dept. of Physiology, Maastricht University, Maastricht, The
11 Netherlands.

12

13 Corresponding author:
14 Ulrich Schotten, MD, PhD
15 Dept. of Physiology
16 Maastricht University
17 PO Box 616
18 6200 MD Maastricht
19 The Netherlands
20 Fax: +31 43 3884166
21 Phone: +31 43 3881077
22 Email: Schotten@maastrichtuniversity.nl
23

24

Condensed abstract

Structural remodeling during atrial fibrillation (AF) not only leads to longitudinal dissociation but also transmural dissociation. A proof-of-principle model was developed to investigate that progressive loss of endo-epicardial electrical connections increases the degree of endo-epicardial electrical activity dissociation which results in an enhanced breakthrough rate and AF stability.

What is New?

- Using this model we could simulate transmural conduction between endocardial and the epicardial layer.
- Decrease in the degree of coupling between endocardium and epicardium increased the degree of endo-epicardial electrical activation dissociation and paradoxically increased the incidence of transmural conduction until a certain degree of connectivity.
- Endo-epicardial electrical activity dissociation was the strongest determinant of AF persistence in all done simulations.

Abstract

Aims: Loss of side-to-side electrical connections between atrial muscle bundles is thought to underlie conduction disturbances predisposing to atrial fibrillation (AF). Putatively, disruption of electrical connections occurs not only within the epicardial layer but also between the epicardial layer and the endocardial bundle network, thus impeding transmural conductions (“breakthroughs”). Paradoxically, both clinical and experimental studies have shown an enhancement of breakthroughs during later stages of AF. We tested the hypothesis that endo-epicardial uncoupling enhances endo-epicardial electrical dyssynchrony, increases breakthrough rate (BTR) and AF stability.

Methods: In a novel dual-layer computer model of the human atria, 100% connectivity between the two layers served as healthy control. Atrial structural remodeling was simulated by reducing number of connections between layers from 96 to 6 randomly chosen locations.

Results: With progressive elimination of connections, AF stability increased. Reduction of the number of connections from 96 to 24 resulted in an increase in endo-epicardial dyssynchrony from $6.6 \pm 1.9\%$ to $24.6 \pm 1.3\%$, with a concomitant increase in BTR. A further reduction to 12 and 6 resulted in more pronounced endo-epicardial dyssynchrony of $34.4 \pm 1.15\%$ and $40.2 \pm 0.52\%$ but with BTR reduction. This biphasic relationship between endo-epicardial coupling and BTR was found independently from whether AF was maintained by reentry or ectopic focal discharges.

Conclusions: Loss of endo-epicardial coupling increases AF stability. There is a biphasic relation between endo-epicardial coupling and BTR. While at high degrees of endo-epicardial connectivity the BTR is limited by the endo-epicardial synchronicity, at low degrees of connectivity it is limited by number of endo-epicardial connections.

Key Words: Atrial Fibrillation – Computer Model – Transmural Conduction – Electrical Dissociation - Ectopic Focal Discharges

Abbreviations:

AF = atrial fibrillation; **PS** = phase singularities; **BTR** = breakthrough rates; **AFCL** = atrial fibrillation cycle length; **WFCV** = wave front conduction velocity; **EA** = excitable area; **aAF** = acute atrial fibrillation; **3wAF** = 3 weeks of atrial fibrillation; **6mAF** = 6 months of atrial fibrillation

Introduction

Several mechanisms have been suggested to explain the increasing stability of atrial fibrillation (AF) over time. Disruption of electrical coupling between muscle bundles, resulting in narrower and thus more fibrillation waves, is considered as one of the main mechanisms contributing to AF stability in structurally remodeled atria.¹⁻⁴ The anatomy of the atrial wall has been demonstrated to significantly determine conduction patterns of fibrillation waves during AF.⁵ For example, Gray et al. showed that the direction of atrial muscle bundles correlates well with the location of block lines and breakthrough in right atrium.⁶ Similarly, Wu et al. demonstrated an effect of pectinate muscles orientation on fibrillation patterns and observed transmural conduction in pectinate muscle area.⁷ De Groot et al. found increases both in number of fibrillation waves and in incidence of epicardial breakthroughs in patients with longstanding AF compared to patients with acute AF,⁸ suggesting that the development of the substrate for AF goes along with increasing incidence of conduction from the sub-epicardial layer to the endocardial bundle network and vice versa. This concept of three-dimensional conduction of fibrillation waves during AF was recently confirmed by several animal studies using simultaneous mapping of the epicardial layer and the endocardial bundle network.^{6,9-11} While these studies conclusively demonstrate transmural conduction in the atrial wall, they leave open several important conceptual questions.

In particular they could not answer the question what drives three-dimensional conduction during AF. In structurally remodeled atria, disruption of electrical connections not only occurs between the muscle bundles within the epicardial layer but also between the epicardial layer and the endocardial bundle network. This should enhance endo-epicardial conduction block and thus impede endo-epicardial conduction. In contrast, the epicardial breakthrough rate is higher in

goats and patients with persistent AF compared to acute AF.^{2, 11, 12} In a previous simulation study,¹³ we used a new dual-layer computer model of AF to address the question whether dissociation of endo-epicardial electrical activity results in increased AF stability. In the present study, we test the hypothesis that progressive loss of endo-epicardial electrical connections increases the degree of endo-epicardial dissociation of electrical activity and that enhanced degree of endo-epicardial dissociation results in an enhanced breakthrough rate and a more complex fibrillation pattern.

Methods

Model

Model structure

A recent study by Eckstein et al. revealed an increase in electrical activity dissociation between epicardial layer and endocardial bundle network due to progressive uncoupling between these two layers.¹⁰ In order to model this phenomenon we chose a novel dual-layer computer model with varying degrees of electrical coupling between two layers (each layer is representation of either the endocardial or the epicardial layer). Each layer was modeled with a mono-domain reaction-diffusion model of a size of $4\text{cm} \times 4\text{cm}$ and composed of 400×400 segments with a size of $0.01\text{cm} \times 0.01\text{cm}$. Since specific connectivity between remodeled epicardial and endocardial layer is not known, we chose a randomly distributed set of circular connection points between both layers. Electrical coupling between the two layers was implemented by adding an Ohmic conductor between opposing segments at so-called connection points. Connection points radius were chosen so that proper transmural conduction was obtained (Figure 1A).¹³

Atrial Cell Model

Ionic currents and calcium handling for each segment was described by the Courtemanche-Ramirez-Nattel model.¹⁴ Conductivities were the same in both directions, $\sigma_x = \sigma_y = 0.5 \text{ mS cm}$, which implies isotropic tissue. Total ionic membrane current was given by;

$$I_{\text{ion}} = I_{\text{Na}} + I_{\text{K1}} + I_{\text{to}} + I_{\text{Kur}} + I_{\text{Kr}} + I_{\text{Ks}} + I_{\text{Ca,L}} + I_{\text{p,Ca}} + I_{\text{NaK}} + I_{\text{NaCa}} + I_{\text{b,Na}} + I_{\text{b,Ca}} \quad (1)$$

where I_{Na} is fast inward Na^+ current, I_{K1} is inward rectifier K^+ current, I_{to} transient outward K^+ current, I_{kur} is ultrarapid delayed rectifier K^+ current, I_{kr} is rapid delayed rectifier current, I_{Ks} is slow delayed rectifier K^+ current, $I_{\text{Ca,L}}$ is L-type Ca^{2+} current, $I_{\text{p,Ca}}$ is Ca^{2+} pump current, I_{NaK} is Na^+ - K^+ pump current, I_{NaCa} is Na^+ / Ca^{2+} exchanger current, and $I_{\text{b,Na}}$ and $I_{\text{b,Ca}}$ are background Na^+ and Ca^{2+} currents. To incorporate changes in ionic currents as observed in atrial fibrillation, conductivities for I_{to} , $I_{\text{Ca,L}}$, and I_{K1} were set at 40%, 35%, and 200% of the default values, respectively.³

Simulation protocols

To demonstrate that the quantitative relation between the breakthrough rate, the degree of endo-epicardial dyssynchrony, and the number of endo-epicardial connections is independent from the mechanisms driving AF, the arrhythmia was maintained by A) spiral waves and B) random focal activation mimicking continuous ectopic focal discharges.

A) AF driven by spiral waves

To investigate the effect of the number of connection points on fibrillatory behavior, the following simulation protocol was applied (Figure 1C):

1. In one layer, a spiral wave was initiated using an S1-S2 protocol,¹⁵⁻¹⁷ while the other layer was quiescent, as described in our previous study.¹³ The simulation was continued for 1 second.
2. One second after the start of the simulation, 6 connection points were added at randomly chosen sites. These sites were chosen such that two connection points were at least 0.15 cm apart. To exclude possible bias resulting from a particular geometry of connection points, 8 different sets of 6 randomly chosen sites were created. For each of the 8 configurations, the simulation of step 1 was continued for 6 more seconds. This resulted in 8 different simulations that were used to initialize the simulations in the next step.
3. The 8 simulations from step 2 were continued for another 6 seconds, either without changing the connection points or after adding randomly chosen connection points (at least 0.15cm apart). Thus, the total number of connections was 6, 12, 24, 48 or 96. In addition, each simulation from step 2 was continued with 100% connectivity, i.e., all opposing segments in the two layers were connected to each other.

As described above, steps 2 and 3 were performed 8 times such that in total 48 simulation runs were performed in step 3.

B) AF driven by random ectopy

1. The dual layer matrix was paced at randomly chosen pacing sites distributed over both layers. The model was paced at random time steps. The frequency of ectopy was chosen in a way that an AF cycle length around 200ms was achieved.

2. Step 1 was done for all different number of connections (6, 12, 24, 48, 96, and 100% connectivity) for eight randomly distributed connections and simulations continued for 6 seconds.

In our model, 6 and 12 connections represented severely remodeled atria; 24, 48, and 96 connections represented moderately remodeled atria; and 100% connectivity represented a healthy atrium.

Analysis

In all simulations the following parameters were analyzed (for algorithms used for these analyses see supplemental methods):

- Number of phase singularities (PSs)
- Phase singularity lifespan
- Breakthrough rates (BTRs)
- Breakthrough lifespans
- Number of fibrillation waves
- Wave front lifespans
- Atrial fibrillation cycle length (AFCL)
- Wave Front Conduction Velocity (WFCV)
- Excitable area (EA)
- Degree of endo-epicardial dyssynchrony
- Degree of endo-epicardial dissociation
- Atrial fibrillation duration

Results

Figure 2 shows representative simulations of AF driven by spiral waves for different degrees of endo-epicardial connectivity. Snapshots are shown for each 1000ms (see online supplement for videos). When both layers are fully connected (100% connectivity, Figure 2A), the two layers synchronized within 50ms. No BTs were observed and the last depolarization waves disappeared after 2100ms.

In the examples with 96 and 48 connections (Figure 2B-C), the two layers showed rapid synchronization by a high number of BTs. With increasing synchronization of the activity in the two layers, the number of waves, PSs, and BTR decreased. After 2000ms the two layers showed synchronized activity and shortly thereafter, the episode terminated.

In the example with 24 connections (Figure 2D), dyssynchrony decreased between 1000 and 2000ms, which resulted in synchronized activity between 3000 and 4000ms and termination of the episode at 4100ms.

In the examples with 12 and 6 connections (Figure 2E-F), the initial rate of BTs is lower, no resynchronization of the two layers occurred, dyssynchrony of electrical activation between the two layers remained high, and the fibrillation patterns in both layers remained complex.

In none of the simulations of AF driven by random ectopy, spiral wave initiation was observed. Propagation patterns remained organized and only consisted of either radial spread of ectopic waves or breakthroughs (Figure 3).

Parameters determining stability of AF

Figure 4 shows the Kaplan-Meier curve of AF persistence in the set of 48 spiral waves driven simulations. With a progressive loss of connections, AF persistence strongly increased.

In order to study how loss of connectivity stabilizes AF, the effect of the number of connections on a variety of parameters describing the substrate for AF was studied.

Figure 5 shows the relation between the connectivity and number of phase singularities, phase singularity lifespan, breakthrough rates, breakthrough lifespan, number of waves and wave front lifespan, and electrophysiological parameters such as wave front conduction velocity (WFCV), AF cycle length (AFCL), excitable area (EA), breakthrough rate (BTR), and endo-epicardial dyssynchrony. The numbers of PSs at 24 and 96 connections were significantly higher compared to 100% connectivity. Consequently, PS lifespan at 24 connections and 96 connections were significantly shorter than at 100% connectivity ($p < 0.05$) (Figure 5A-B). As illustrated in Figure 5C-D, BTRs showed an increase with reduction of connections down to 24 connections, but with a further elimination of connections BTR decreased. No significant differences were found in BT lifespan between the groups.

The number of waves was significantly larger at 12, 24, 48, and 96 connections than at 100% connectivity (Figure 5E) while the wave front lifespans were shorter than at 100% connectivity (Figure 5F). There was no significant difference in AFCL, WFCV, and EA between different number of connections (see Figure 5G-I). Dyssynchrony progressively and strongly increased with the elimination of the endo-epicardial connections (Figure 5J).

The same parameters were compared between all episodes that were sustained and those that were not sustained irrespective of the number of connections (Figure 6). This analysis was performed to identify which parameters were associated with AF stability independently from the number of connections.

In panels A and B, the number of PSs and PS lifespans are shown. There were no significant differences between the two groups in these parameters. There were neither differences in BTR

and BT lifespan (panel C and D) nor in the number of waves or wave front lifespan (panel E and F). There were no differences in AFCL and WFCV, but EA was slightly but significantly lower in sustained versus non-sustained AF (panels G, H, and I). The most striking difference was that the degree of dyssynchrony was much higher in the group with sustained AF compared to non-sustained AF (group J).

In order to investigate which parameter is the strongest determinant of AF duration, we used multilevel logistic regression analysis among measured parameters. Three parameters were significantly correlated to AF stability (see Table 1). Of these significant predictive parameters, dyssynchrony was by far the strongest determinant of AF persistence in this set of simulations. In random ectopy driven simulations, AF was sustained by pacing so that a study on AF stability was not applicable.

Relation between dyssynchrony and breakthrough rate

In Figure 7A, dyssynchrony (blue line), BT rate (red line), and BT rate during the first 50ms after adding the connection points are plotted for spiral wave driven AF. The BT rate during the first 50ms after adding the connection points is of interest because in this short time interval the two layers have not yet synchronized and the BT rate largely depends on the number of available endo-epicardial connections. This 'initial' BT rate, decreases with the number of connections (black line). However, the overall BT rate for the whole AF episode showed a biphasic relation to the number of connections, increasing from 100% connectivity down to 24 connections, but decreasing for 12 and 6 connections.

In Figure 7B, dyssynchrony (blue line) and BT rate (red line) extracted from random pacing simulations are illustrated. The overall BT rate of the whole AF episode showed a biphasic

relation to the number of connections, increasing from 100% connectivity down to 24 connections, but decreasing for 12 and 6 connections. This pattern was similar to that observed in our spiral wave driven simulations.

Comparison of experimental data and simulation data

In Figure 8, the BT rate (as percentage of all waves) is plotted against the degree of dissociation for experimental^{10, 19} and simulation data extracted from spiral waves driving simulations. For this analysis, dissociation was calculated both for modeling data and experimental data as previously described.^{10, 19}

Experimental data (open squares) includes data derived from goats in acute AF (aAF, n=7), 3 weeks of AF (3wAF, n=7), and 6 months of AF (6mAF, n=7) and were taken from a previous study.¹⁹ As illustrated in this figure, the degree of endo-epicardial dissociation increased with AF duration. To some extent of dissociation, increase in degree of dissociation leads to increase in BT both in experimental (3wAF) and modeling (24 connections). Beyond that, even with huge increase in dissociation only slight increase in BT rate in experimental (6mAF) and decrease in modeling (12 connections) result was observed. Overall, although there was not point to point match between experimental and modeling results but patterns were similar.

Discussion

The mechanisms contributing to an increase in stability of AF are not fully understood. Electrical remodeling, electrical uncoupling between muscle bundles and heterogeneity of action potential duration all together leading to local conduction heterogeneities have been hypothesized to increase stability of AF.^{2, 20} More specifically, disruption of electrical side-to-side connections

between muscle bundles occurs as a consequence of structural alterations in the atrial wall.¹ This loss of connectivity between muscle bundles leads to an enhanced likelihood of conduction block, increasing the number of fibrillation waves and putatively to increasing AF stability.^{2, 12} Disruption of electrical side-to-side connections does not only occur within the epicardial layer but most likely also between the epicardial layer and the endocardial bundle network.^{10, 11} This uncoupling between the epi- and endocardial layers of the atrial wall – at a first glance – should lead to less transmural conduction events resulting in a lower incidence of breakthrough during AF. On the contrary, in goats as well as in patients the incidence of breakthroughs has been shown to be much higher in persistent than in acute forms of the arrhythmia.^{2, 8, 10, 19} The present study was undertaken to clarify how loss of endo-epicardial connectivity might result in more transmural conduction and higher breakthrough rates. We hypothesized that disruption of endo-epicardial connections increases the dissociation of electrical activity between the epicardial layer and the endocardial muscle bundles. As a prerequisite for transmural conduction, increased endo-epicardial dissociation of electrical activity will enhance transmural conduction and result in a higher breakthrough rate despite lower availability of endo-epicardial connections and, as a consequence, an increase in AF duration.

We chose a simplified geometry model to assess the dynamics of transmural conduction in presence of endo-epicardial dissociation. Rational of choosing this simplified structure is to avoid complexities which makes us unable to investigate this specific dynamical property because of huge computational load and parameters space associated with structurally realistic model.

We used our recently described dual-layer computer model of AF consisting of two 2D sheets of excitable tissue connected through a variable number of electrical interconnections.¹³ In a proof-

of-principle study in this model we investigated the quantitative relation between the number of endo-epicardial connections (degree of endo-epicardial connectivity), endo-epicardial dissociation of electrical activity, breakthrough rate, and stability of AF.

Effect of transmural uncoupling on dyssynchrony and breakthroughs

There are two groups of atrial models with respect to geometrical properties: surface models which treat the atria as two dimensional sheet folded into the shape of the atria (with two main cavities, atrial appendages, and connections between the two atria at the septal rings)²²⁻²⁴ and the true 3D volumetric models. Volumetric models go into greater detail in modeling the atria including such properties as complex anatomy of endocardium bundle networks²⁵⁻²⁸ and fiber orientations in atrium.²⁹⁻³¹ Several mechanisms were investigated using volumetric models such as effect of ectopies, AP heterogeneities, fibrosis and meandering of phase singularities on fibrillatory propagation patterns and AF stability. A few recent studies also investigated the effect of atrial wall thickness of fibrillatory patterns and on AF maintenance.^{9, 21}

While all these models were useful to answer many important questions about mechanisms contributing to AF stability none of them considered endo-epicardial dyssynchrony, transmural conduction, and their effect on AF stability.

The present study was designed to investigate relationship between breakthrough incidences, endo-epicardial dyssynchrony and AF stability. We chose dual layer model instead of volumetric 3D model because: (i) The exact location and distribution of muscle bundles providing endo-epicardial electrical connections is very difficult to determine experimentally. Any simulation implementing a detailed anatomy of such endo-epicardial connection points would suggest a level of accuracy that can currently not be achieved even with advanced imaging techniques. (ii)

We aimed to exclusively focus on properties of endo-epi dissociation without confounding effect of complex 3D geometry, which due to scope and complexity could not be addressed in this study.

The novelty of our model is that it describes truly three-dimensional (transmural) conduction between the endocardial and the epicardial layer¹³ and by doing so introduces a new type of simulated fibrillation waves, i.e. breakthroughs. In the present study we tested how endo-epicardial uncoupling affects endo-epicardial dissociation and breakthrough rate. We demonstrate that a decrease in the degree of coupling between endocardium and epicardium increased the degree of dyssynchrony and paradoxically increased the incidence of transmural conduction until a certain degree of connectivity. In other words, although a reduction in the number of connections between two layers decreases the number of available transmural electrical pathways, the incidence of transmural conduction increases. Our results demonstrate that this paradox can be explained by the enhanced dyssynchrony between the two layers. If both opposing layers at a connection point are either excited or non-excited, no transmural conduction occurs. Only in the presence of dyssynchronous electrical activity, fibrillation waves can propagate along endo-epicardial connections. As a result, in the presence of a high number of connections the breakthrough rate is low because the degree of endo-epicardial dissociation is low, despite the fact that the number of available endo-epicardial connections is high. Interestingly, increasing the extent of uncoupling to a larger degree (fewer than 24 connections) showed an opposite effect. The breakthrough rate decreased with further decrease in the number of connections while the degree of dyssynchrony increased. To explain this phenomenon, we measured the breakthrough rate during a short period just after introducing more connections (i.e. the start of step 3 in figure 2), when the layers have not yet synchronized. During this period

we calculated the number of BTs during highest achieved degree of dyssynchrony. Under these circumstances, we observed that the breakthrough rate strongly and monotonously declined with a reduction of the number of endo-epicardial connections, just as expected based on the simple reasoning that reduced number of available electrical pathways should reduce the occurrence of endo-epicardial conduction. The results indicate that under these modeling conditions the BT rate not only depends on the degree of dyssynchrony, but also is limited by the actual number of endo-epicardial connection points. In case only a few connections exist between the two layers, breakthroughs will occur less frequently, because of the low number of available endo-epicardial connections, despite a high degree of endo-epicardial dissociation.

We also showed that our conclusions are transferable to circumstances under which AF is maintained but other mechanisms. We tested the proposed relation between endo-epicardial connections, endo-epicardial dissociation and breakthrough rate in a modification of the model in which the arrhythmia is driven by multiple ectopic foci. This mechanism has been shown to perpetuate AF under specific circumstances, such as vagal nerve stimulation.³³ Under these conditions, we identified exactly the same pattern in the quantitative relation between number of endo-epicardial connection points, endo-epicardial dissociation and breakthrough rate.

Effect of transmural uncoupling on AF stability

In this study, we demonstrate that a decrease in transmural coupling increases AF episode stability in spiral waves driven simulations. Importantly, not all of the important determinants of AF stability were altered by the different degrees of endo-epicardial coupling. There was no change in conduction velocity or AF cycle length. Only the excitable area was slightly but significantly affected. Importantly, all differences between small and large degrees of uncoupling

we observed were related to three-dimensional conduction. At a high degree of uncoupling, endo-epicardial dyssynchrony and dissociation were more pronounced, the breakthrough rate increased until certain degree of dyssynchrony. Importantly, AF duration increased with decreasing number of connections and we identified dyssynchrony as the strongest predictor for AF stability. Taken together, these findings clearly suggest that the three-dimensional character of the conduction pattern in itself is an important determinant of the stability of the arrhythmia.

Relation between experimental results and the model data

The phenomenon of endo-epicardial dissociation of electrical activity has experimentally been studied by several research groups. Schuessler et al.³² were the first to reveal endo-epicardial dyssynchrony of activation during acetylcholine-induced AF in canine right atria. Gray et al. and Wu et al. also investigated the three-dimensional structure of the atria and its effect on activation sequences during atrial fibrillation and also observed transmural conduction incidences.^{6,7} Everett et al. compared epicardial direct contact electrograms with non-contact mapping endocardial electrograms and found larger endo-epicardial activation time differences in a rapid atrial pacing model than in control animals.³⁴ Also the elegant study of Yamazaki et al. demonstrated the occurrence of endo-epicardial dissociation during AF in sheep with atrial dilatation.⁹ Recently, Eckstein et al. demonstrated that the degree of endo-epicardial dissociation increases during the course of AF.^{10, 11} The mechanism of this increasing dissociation of electrical activity was not related to endo-epicardial dispersion of refractoriness but rather to loss of endo-epicardial coupling between muscle bundles. Very recently, we demonstrated that loss of continuity in the epicardial layer and anatomical rearrangement of atrial muscle bundles also

contribute to the increase in endo-epicardial dissociation during the development of persistent AF.^{5, 18}

Our modeling data to some extent showed similar pattern with several experimental and clinical studies published during the past years. Both in patients and in goats, enhanced rates of breakthrough have been demonstrated in persistent AF compared to acute AF.⁸ A direct comparison with a previous study by Eckstein et al.^{10, 19} showed a comparable relationship between endo-epicardial dissociation and breakthrough rate, supporting the pathophysiological relevance of our computer model. Both studies show that at low degrees of endo-epicardial dissociation the breakthrough rate is low. At moderate levels of endo-epicardial dissociations the breakthrough rate increases. Interestingly, a further increase in endo-epicardial dissociation (above 50%) only leads to small increase in breakthrough rates in experimental study but decrease in modeling study. Thus, in the range of physiological degrees of endo-epicardial uncoupling, the degree of endo-epicardial dissociation rather than the number of available endo-epicardial electrical connections is the limiting factor for the breakthrough rate.

Study limitations

Our simplified dual-layer model should be considered as a proof-of-principle model. This model does not reflect complex structure of the atrium with pulmonary veins, valve heterogeneity in ionic membrane currents, and variability in atrial wall thickness. Despite these limitations, we have shown that our model is well-suited to investigate the relation between of endo-epicardial dissociation and breakthroughs on AF complexity and stability. How additional complexities in the anatomy of the atrial wall affect endo-epicardial dissociation and transmural conduction should be addressed in future studies.

Funding

This work was supported by the Leducq Foundation (07 CVD 03), the Dutch Research Organization (NWO, VIDI-grant 016.086.379), and the European Network for Translational Research in AF (FP7 collaborative project EUTRAF, No 261057)

Acknowledgements:

This study was supported by a grant from the European Union (FP7 Collaborative project EUTRAF, 261057).

References:

1. Spach MS, Dolber PC. Relating extracellular potentials and their derivatives to anisotropic propagation at a microscopic level in human cardiac muscle. Evidence for electrical uncoupling of side-to-side fiber connections with increasing age. *Circ Res* 1986;58:356-371.
2. Verheule S, Tuyls E, van Hunnik A, Kuiper M, Schotten U, Allessie M. Fibrillatory conduction in the atrial free walls of goats in persistent and permanent atrial fibrillation. *Circ Arrhythm Electrophysiol* 2010;3:590-599.
3. Schotten U, Verheule S, Kirchhof P, Goette A. Pathophysiological mechanisms of atrial fibrillation: a translational appraisal. *Physiological reviews* 2011;91:265-325.
4. Verheule S, Eckstein J, Linz D, Maesen B, Bidar E, Gharaviri A, et al. Role of endo-epicardial dissociation of electrical activity and transmural conduction in the development of persistent atrial fibrillation. *Prog. Biophysics and molecular biology* 2014;15:173–185.
5. Maesen B, Zeemering S, Afonso C, Eckstein J, Burton RA, van Hunnik A, et al. Rearrangement of atrial bundle architecture and consequent changes in anisotropy of conduction constitute the 3-dimensional substrate for atrial fibrillation. *Circ Arrhythm Electrophysiol* 2013;6:967-975.
6. Gray RA, Pertsov AM, Jalife J. Incomplete reentry and epicardial breakthrough patterns during atrial fibrillation in the sheep heart. *Circulation* 1996;94:2649-2661.
7. Wu TJ, Yashima M, Xie FG, Athill CA, Kim YH, Fishbein MC, et al. Role of pectinate muscle bundles in the generation and maintenance of intra-atrial reentry - Potential implications for the mechanism of conversion between atrial fibrillation and atrial flutter. *Circ Res* 24 1998;83:448-462.
8. de Groot NM, Houben RP, Smeets JL, Boersma E, Schotten U, Schalij MJ, et al. Electropathological substrate of longstanding persistent atrial fibrillation in patients with structural heart disease: epicardial breakthrough. *Circulation* 2010;122:1674-1682.

9. Yamazaki M, Mironov S, Taravant C, Brec J, Vaquero LM, Bandaru K, et al. Heterogeneous atrial wall thickness and stretch promote scroll waves anchoring during atrial fibrillation. *Cardiovasc Res* 2012;94:48-57.
10. Eckstein J, Maesen B, Linz D, Zeemering S, van Hunnik A, Verheule S, et al. Time course and mechanisms of endo-epicardial electrical dissociation during atrial fibrillation in the goat. *Cardiovasc Res* 2011;89:816-824.
11. Eckstein J, Zeemering S, Linz D, Maesen B, Verheule S, van Hunnik A, et al. Transmural Conduction is the Predominant Mechanism of Breakthrough during Atrial Fibrillation: Evidence from Simultaneous Endo-epicardial High Density Activation Mapping. *Circ Arrhythm Electrophysiol* 2013; 6(2):334-41.
12. Allesie MA, de Groot NM, Houben RP, Schotten U, Boersma E, Smeets JL, et al. Electropathological substrate of long-standing persistent atrial fibrillation in patients with structural heart disease: longitudinal dissociation. *Circ Arrhythm Electrophysiol* 2010;3:606-615.
13. Gharaviri A, Verheule S, Eckstein J, Potse M, Kuijpers N, Schotten U. A computer Model of Endo-Epicardial Dissociation and Transmural Conduction During Atrial Fibrillation. *Europace* 2012; 14 Suppl 5:v10-v16.
14. Courtemanche M, Ramirez RJ, Nattel S. Ionic mechanisms underlying human atrial action potential properties: insights from a mathematical model. *The American journal of physiology* 1998;275:H301-321.
15. Leon LJ, Roberge FA, Vinet A. Simulation of two-dimensional anisotropic cardiac reentry: effects of the wavelength on the reentry characteristics. *Ann Biomed* 1994;22:592-609.
16. Kuijpers NH, Keldermann RH, Arts T, Hilbers PA. Computer simulations of successful defibrillation in decoupled and non-uniform cardiac tissue. *Europace* 2005;7 Suppl 2:166-177.
17. Kuijpers NH, Keldermann RH, ten Eikelder HM, Arts T, Hilbers PA. The role of the hyperpolarization-activated inward current I_f in arrhythmogenesis: a computer model study. *IEEE Trans Biomed Eng* 2006;53:1499-1511.

18. Verheule S, Tuyls E, Gharaviri A, Hulsmans S, van Hunnik A, Kuiper M, et al. Loss of continuity in the thin epicardial layer due to endomyxial fibrosis increases the complexity of atrial fibrillatory conduction. *Circ Arrhythm Electrophysiol* 2013;6(1):202-11.
19. Eckstein J. Three-Dimensional Substrate of Atrial Fibrillation in the Goat: A Simultaneous Endo-epicardial Mapping Study. Maastricht: Physiology Department, Maastricht University; 2012.
20. Berenfeld O, Zaitsev AV, Mironov SF, Pertsov AM, Jalife J. Frequency-dependent breakdown of wave propagation into fibrillatory conduction across the pectinate muscle network in the isolated sheep right atrium. *Circ Res* 14 2002;90:1173-1180.
21. Kuijpers NH, Potse M, van Dam PM, ten Eikelder HM, Verheule S, Prinzen FW, et al. Mechano-electrical coupling enhances initiation and affects perpetuation of atrial fibrillation during acute atrial dilation. *Heart Rhythm* 2011;8:429-436.
22. Uldry L, Virag N, Lindemans F, Vesin JM, Kappenberger L. Atrial septal pacing for the termination of atrial fibrillation: study in a biophysical model of human atria. *Europace* 2012;14 Suppl 5:v112-v120.
23. Haissaguerre M, Lim KT, Jacquemet V, Rotter M, Dang L, Hocini M, et al. Atrial fibrillatory cycle length: computer simulation and potential clinical importance. *Europace* 2007;9 Suppl 6:vi64-70.
24. Ruchat P, Dang L, Schlaepfer J, Virag N, von Segesser LK, Kappenberger L. Use of a biophysical model of atrial fibrillation in the interpretation of the outcome of surgical ablation procedures. *Eur J Cardiothorac Surg* 2007;32:90-95.
25. Aslanidi OV, Colman MA, Stott J, Dobrzynski H, Boyett MR, Holden AV, et al. 3D virtual human atria: A computational platform for studying clinical atrial fibrillation. *Prog Biophys Mol Biol* 2011;107:156-168.
26. Colman MA, Aslanidi OV, Kharche S, Boyett MR, Garratt CJ, Hancox JC, et al. Pro-arrhythmogenic Effects of Atrial Fibrillation Induced Electrical Remodelling- Insights from 3D Virtual Human Atria. *J Physiol* 2013;591:4249-72.

27. Vigmond EJ, Ruckdeschel R, Trayanova N. Reentry in a morphologically realistic atrial model. *J Cardiovasc Electrophysiol* 2001;12:1046-1054.
28. Gong YF, Xie F, Stein KM, Garfinkel A, Cuianu CA, Lerman BB, et al. Mechanism underlying initiation of paroxysmal atrial flutter/atrial fibrillation by ectopic foci - A simulation study. *Circulation* 2007;115:2094-2102.
29. Zhao J, Butters TD, Zhang H, Pullan AJ, LeGrice IJ, Sands GB, et al. An image-based model of atrial muscular architecture: effects of structural anisotropy on electrical activation. *Circ Arrhythm Electrophysiol* 2012;5:361-370.
30. Krueger MW, Severi S, Rhode K, Genovesi S, Weber FM, Vincenti A, et al. Alterations of atrial electrophysiology related to hemodialysis session: insights from a multiscale computer model. *J Electrocardiol* 2011;44:176-183.
31. Kharche S, Seemann G, Margetts L, Leng J, Holden AV, Zhang HG. Simulation of clinical electrophysiology in 3D human atria: a high-performance computing and high-performance visualization application. *Concurr Comp-Pract E* 2008;20:1317-1328.
32. Schuessler RB, Kawamoto T, Hand DE, Mitsuno M, Bromberg BI, Cox JL, et al. Simultaneous epicardial and endocardial activation sequence mapping in the isolated canine right atrium. *Circulation* 1993;88:250-263.
33. Lee S, Sahadevan J, Khrestian CM, Durand DM, Waldo AL. High density mapping of atrial fibrillation during vagal nerve stimulation in the canine heart: restudying the Moe hypothesis. *J Cardiovasc Electrophysiology* 2013;24(3):328-335
34. Everett TH 4th, Wilson EE, Hulley GS, Olgin JE. Transmural characteristics of atrial fibrillation in canine models of structural and electrical atrial remodeling assessed by simultaneous epicardial and endocardial mapping. *Heart Rhythm* 2010;7:506-517.

Figure 1. Dual layer model of the atrial wall (A) Model structure with two layers (epi- and endocardium) and transmural connections (grey cylinders). (B) Dissociation of electrical activity between the two layers and transmural conduction resulting in a breakthrough wave (black arrow). (C) Simulations protocol (see methods section for details).

Figure 2. Colour-coded membrane potentials of representative spiral wave driven simulations with different degrees of endo-epicardial electrical coupling. The epicardial layer is shown in the top, the endocardial in the bottom panel. Snapshots are shown for every second of simulation time.

Figure 3. Colour-coded membrane potentials of representative of AF simulations driven by random ectopy with different degrees of endo-epicardial electrical coupling. The epicardial layer is shown in the top, the endocardial in the bottom panel. Snapshots are shown for every second of simulation time. The black in the upper panel at 2000ms is showing an ectopy. The arrow in the lower panel at 1000ms is showing a BT.

Figure 4. AF persistence. Kaplan-Meier curve showing atrial fibrillation persistence in different sets of simulations with 6, 12, 24, 48, 96 connections, and 100% connectivity (n = 8 for all different sets of simulations).

Figure 5. Electrophysiological parameters as a function of the degree of connectivity. Averages for the whole simulation period (6000 ms) are shown for all parameters. A) Average number of PSs; B) PS lifespan; C) Average breakthrough rates; D) Breakthrough lifespan; E) Average

number of waves; F) Wave front lifespan. G) Average AF cycle lengths; H) Average wave front conduction velocity; I) Average excitable area; J) Average degree of dyssynchrony.

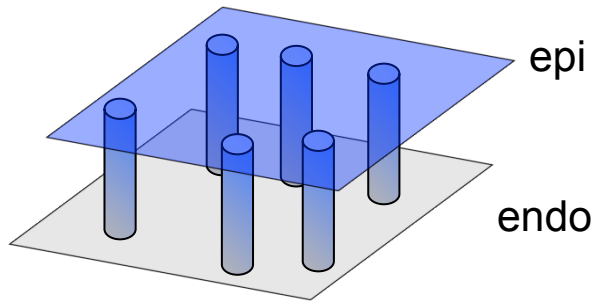
Figure 6. Differences in electrophysiological parameters between non-sustained (<6 sec) and sustained AF episodes. All parameters were averaged for the entire durations the AF episodes. A) Average number of PSs; B) PS lifespan; C) Average breakthrough rates; D) Breakthrough lifespan; E) Average number of waves; F) Wave front lifespan; G) Average AF cycle lengths; H) Average wave front conduction velocity; I) Average excitable area; J) Average degree of dyssynchrony.

Figure 7. A) Relation of BTR and dyssynchrony to the degree of epi-endo connectivity in spiral wave driven simulations. Average percentage of dyssynchrony (blue) over the entire period of each simulation. Average BTR over the entire duration of the episodes (red) and within the first 50ms (black, highest degree of dyssynchrony). B) Relation of BTR and dyssynchrony to the degree of epi-endo connectivity in simulations of AF driven by random ectopy. Average percentage of dyssynchrony (blue) over the entire period of each simulation. Average BTR over the entire duration of the episodes (red).

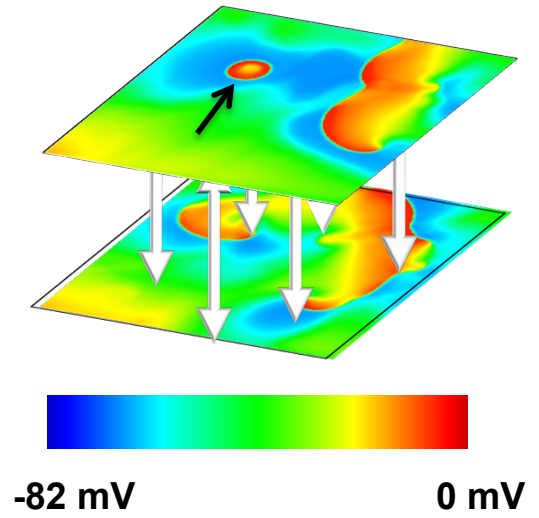
Figure 8. Comparison of modeling data with experimental results. Breakthrough rates (as percentage of all waves) versus the degree of dissociation observed in experimental (red squares) and simulation studies (blue squares). Abbreviations: con: number of connections in simulation studies; aAF: goats in acute AF; 3mAF: goats after 3 weeks of AF; 6mAF: goats after 6 months of AF.

Figure 1

A



B



C

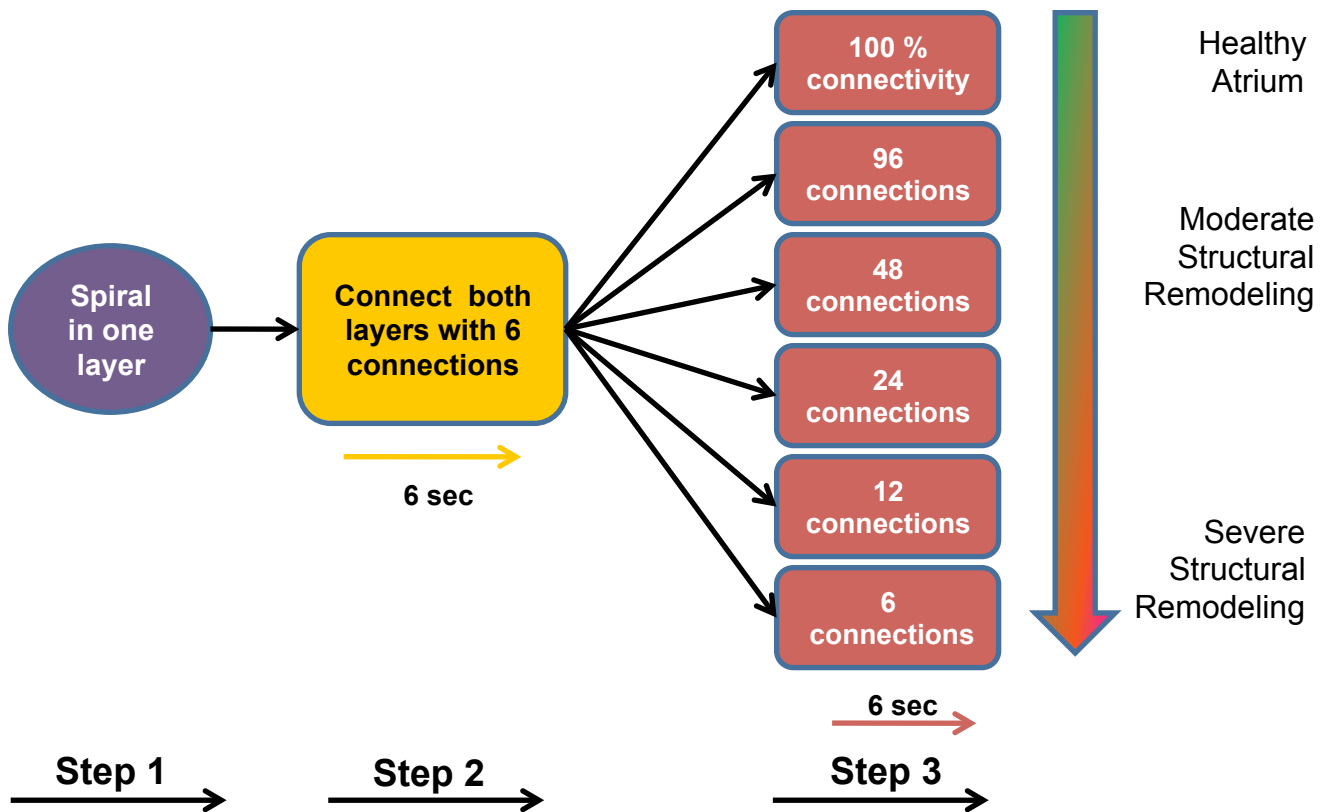


Figure 2

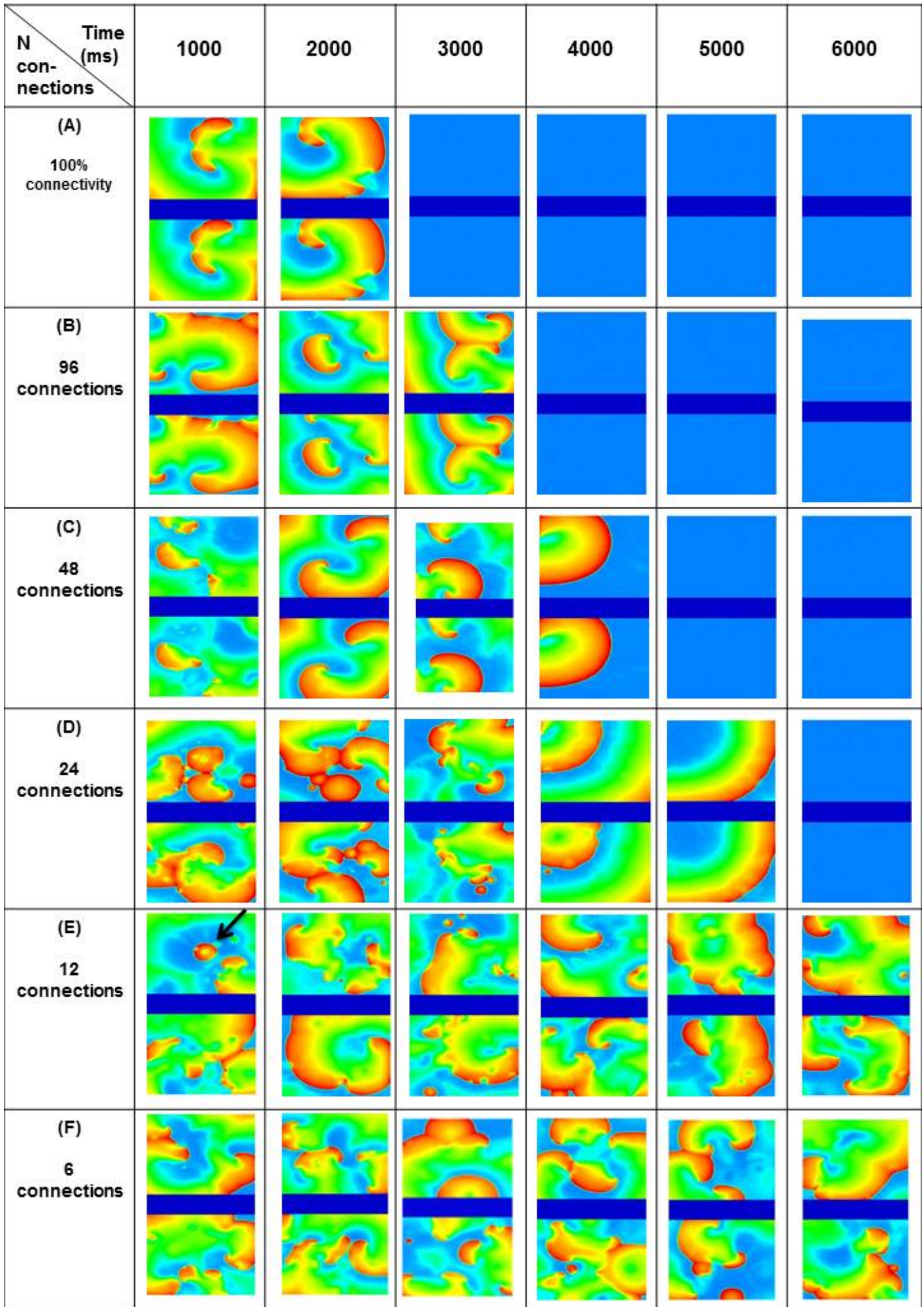


Figure 3

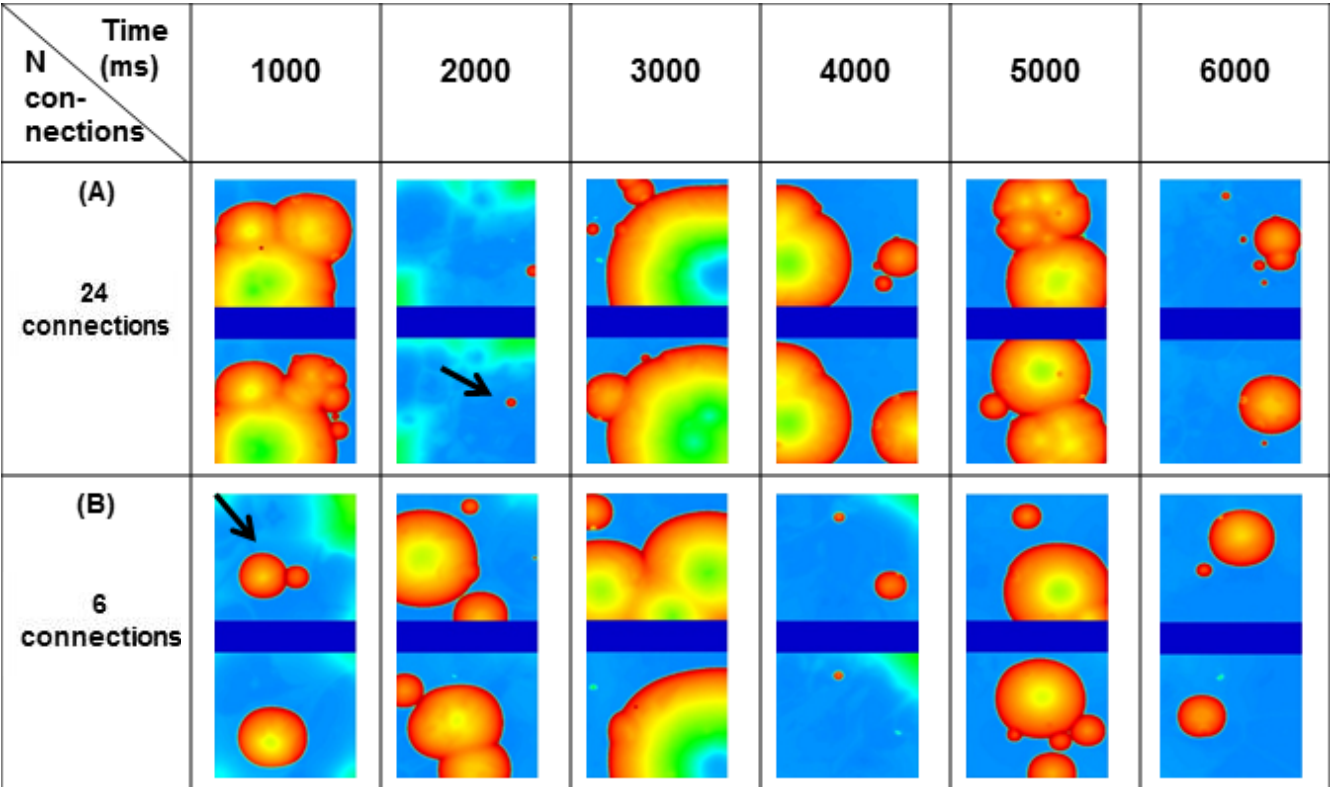


Figure 5

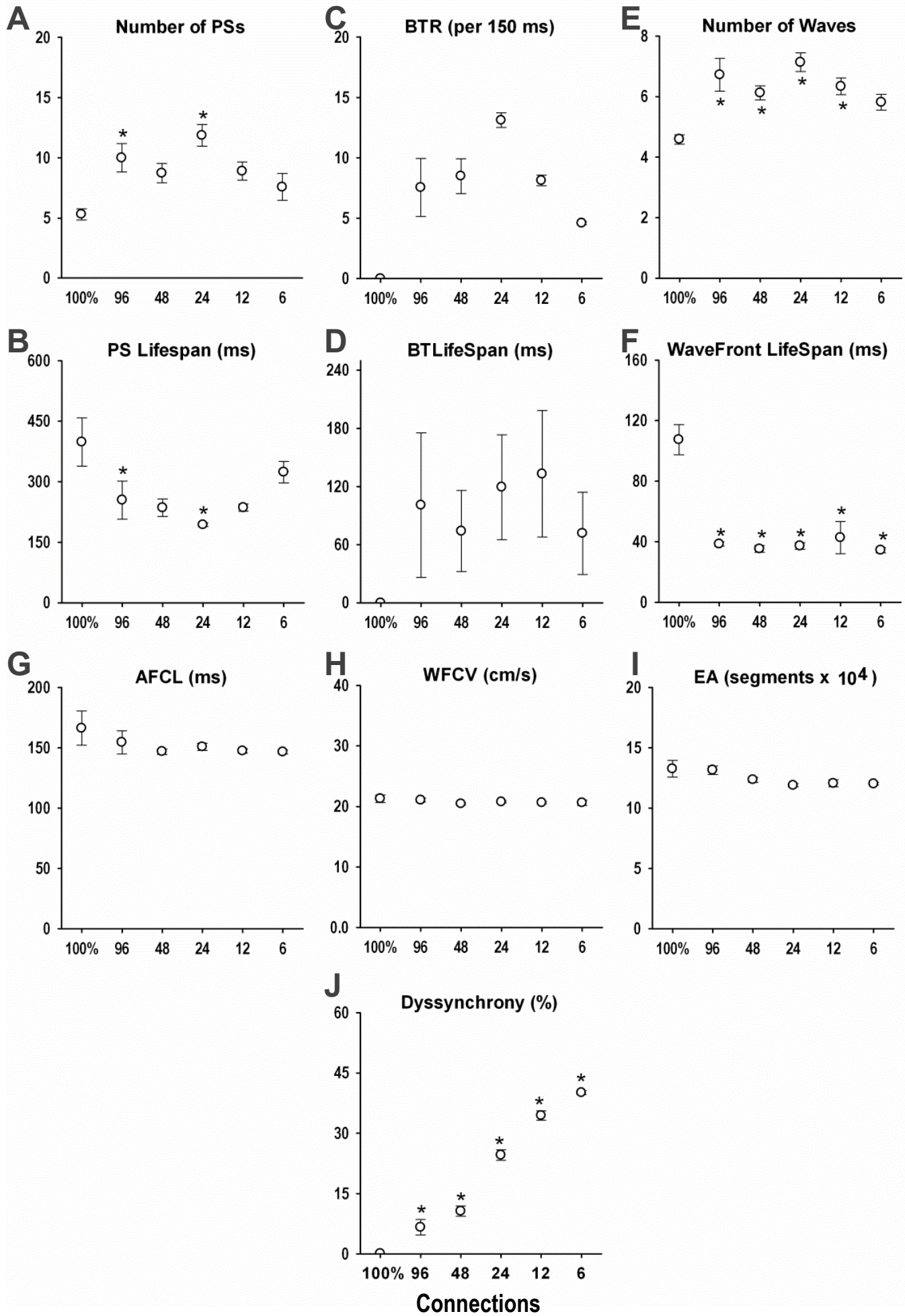


Figure 6

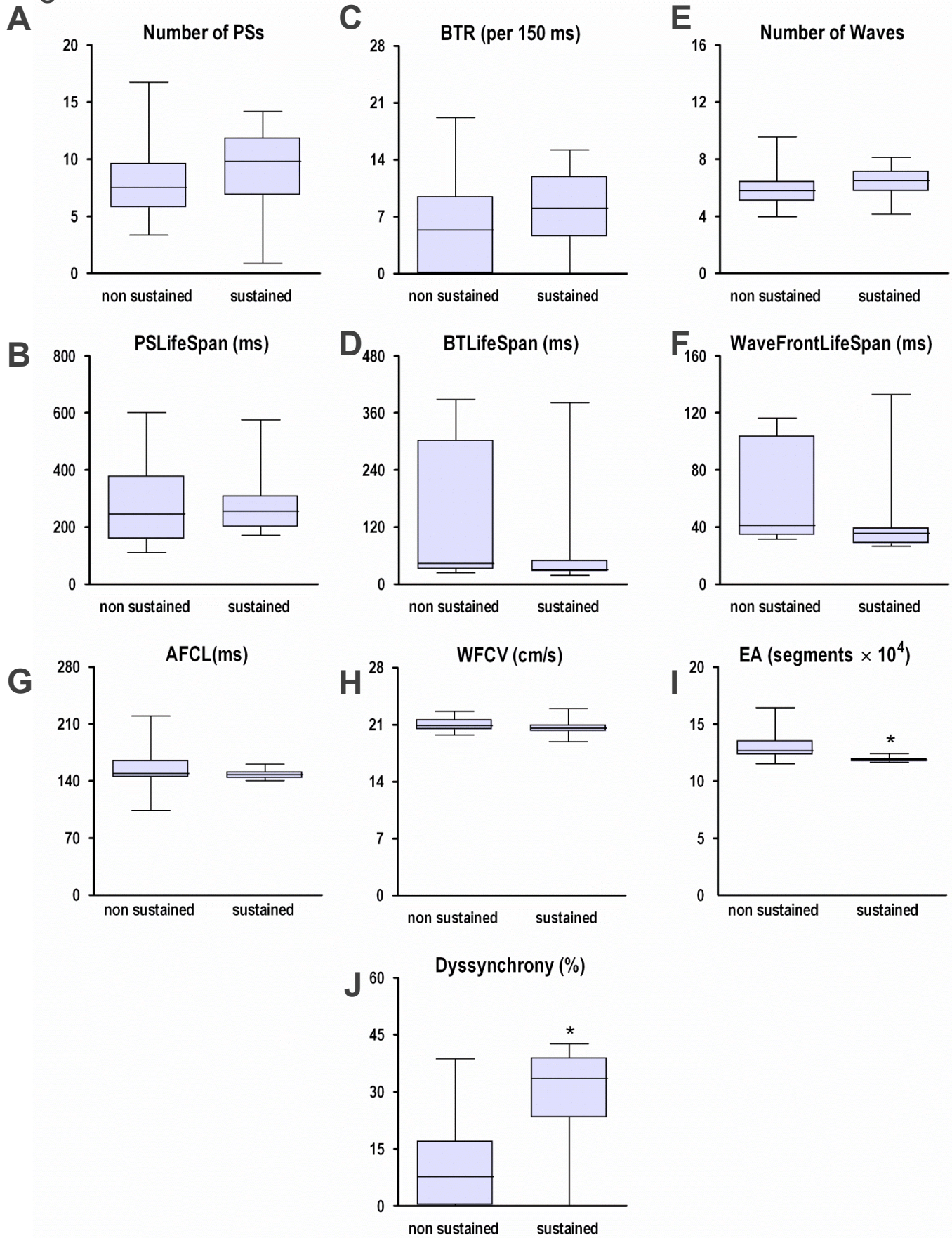


Figure 7

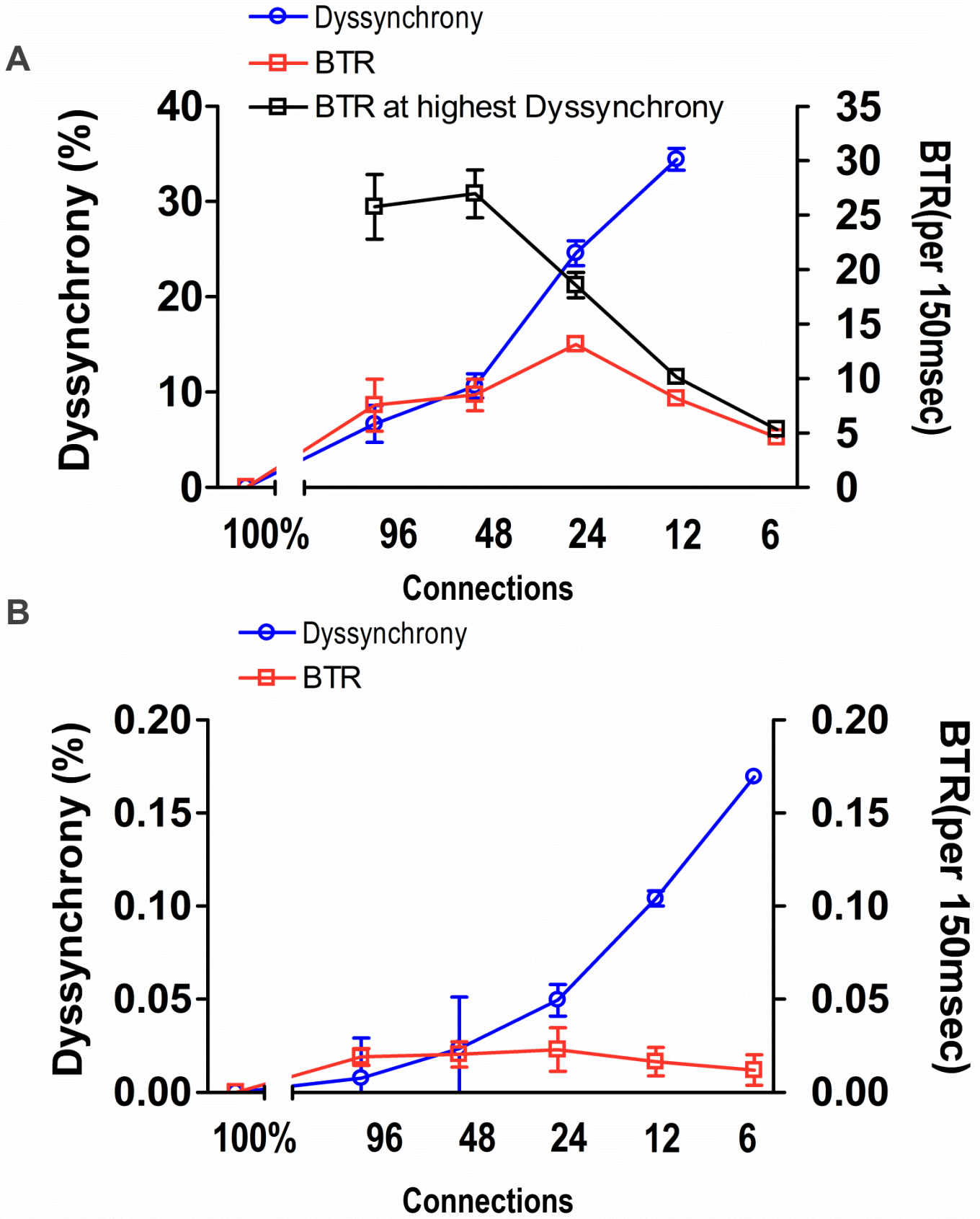


Figure 8

